한국기계가공학회지, 제20권, 제7호, pp. 15～24(2021.07) ISSN 1598-6721(Print)
Journal of the Korean Society of Manufacturing Process Engineers, Vol. 20, No. 7, pp. 15~24(2021.07) ISSN 2288-0771(Online)

https://doi.org/10.14775/ksmpe.2021.20.07.015

Analysis of Environmental Factors Affecting the Machining Accuracy

Young Bok Kim[*,**], Wee Sam Lee[*], June Park[*], Yeon Hwang[*], and June Key Lee[**,#]

[*]Intelligent Optical Module Research Center, KOPTI., [**]Department of Materials & Engineering, Chonnam National UNIV.

가공정밀도에 영향을 미치는 환경요소 분석

김영복[*,**], 이의삼[*], 박준[*], 황연[*], 이준기[**,#]

[*]한국광기술원 지능형광학모듈연구센터, [**]전남대학교 신소재공학부

(Received 11 April 2021; received in revised form 06 May 2021; accepted 10 May 2021)

ABSTRACT

In this paper, to analyze the types of surface morphology error according to factors that cause machining error, the experiments were conducted in the ultra-precision diamond machine using a diamond tool. The factors causing machining error were classified into the pressure variation of compressed air, external shock, tool errors, machining conditions (rotational speed and feed rate), tool wear, and vibration. The pressure variation of compressed air causes a form accuracy error with waviness. An external shock causes a ring-shaped surface defect. The installed diamond tool for machining often has height error, feed-direction position error, and radius size error. The types of form accuracy error according to the tool's errors were analyzed by CAD simulation. The surface roughness is dependent on the tool radius, rotational speed, and feed rate. It was confirmed that the surface roughness was significantly affected by tool wear and vibration, and the surface roughness of Rz 0.0105 ㎛ was achieved.

Key Words : Ultra-precision Diamond Machining(초정밀가공), Pressure Strain(압력변형), Vibration(진동), Diamond Tool(다이아몬드 공구), Form Accuracy(형상정밀도), Surface Roughness(표면거칠기)

1. Introduction

In recent years, there has been increasing demand for integrating camera modules into portable appliances and autonomous cars. In this context, we note that optical lenses are a key component of camera modules. Although spherical glass lenses have been commonly used in earlier cameras, the usage of aspherical plastic lenses has attracted increasing attention as they offer the benefits of high functionality, increased pixel number, compactness, and low costs. In the injection-mold-based fabrication of aspherical plastic lenses, the ultra-precision cutting process using a diamond tool has been mainly applied for the mold core's machining method.[1] With industrial development, the precision required for fabricating optical lenses has steadily risen. In the

Corresponding Author : junekey@jun.ac.kr
Tel: +82-62-530-1692, Fax: +82-53-581-2295

mold-machining process for optical lenses, form accuracy and surface roughness are the most important measurement-assessment parameters, and therefore, numerous studies have been carried out to optimize these parameters. The form accuracy is defined as the difference from the designed shape. In the study to optimize the form accuracy of the machined surface, the method of compensating the tool-path trajectory was mainly studied.[2] Meanwhile, the surface roughness is significantly affected by variables that are difficult to control, such as vibration and tool wear, [3,4]and thus, it is difficult to improve the surface roughness without removing the underlying causes. As regards improving the surface roughness, various studies have focused on minimizing the chattering of tools and workpieces,[5,6] tool-wear minimization,[7] and the optimization of machining conditions (rotation speed, feed rate, and depth of cut).[8,9] However, more studies are required to achieve extreme machining precision with ultra-precision diamond machines that can offer transfer control resolutions of 1 nm.

In this study, we classified the representative environmental factors affecting the machining precision in diamond-tool-based ultra-precision machining and analyzed the types of machining errors corresponding to each factor. The major factors causing the machining errors were determined to be the pressure variation of compressed air, external shock, tool errors, machining conditions (rotation speed and feed rate), tool wear, and vibration.

2. Ultra-precision Diamond Machine and Tools

2.1 Ultra-precision Diamond Machine

The shelf-type ultra-precision diamond machine (model: ASP01-UPX, Nachi-fujikoshi) was used in our experiments as shows in Fig. 1(a). This machine affords five-axis synchronous control (X, Y, Z, B, and C), with transfer control resolution of the main axes (X, Y, and Z) is up to 1.0 nm. The machine was installed in an independent booth specially designed to minimize the effect of vibration in a cleanroom in which temperature and humidity were maintained constant. An active-type vibration isolation system was installed on the floor surface for controlling vibrations.

The granite base was installed on the vibration isolation system, and the major components of the cutting machine were positioned atop this platform. In this machine, the X- and Z-axes are orthogonal to each other, and the non-friction structured slide is transferred along a guideway by means of oil hydrostatic bearings. A B-axis rotary table, which can rotate 360° through the guideway of the oil hydrostatic bearing, is installed on the X-axis.

The Y-axis for the control of up and down movement is orthogonal to the Z-axis. An encoder-type air-bearing work spindle of the C-axis is installed orthogonal to the Y-axis.

2.2 Diamond Tool

In the mold-core cutting process for manufacturing optical lenses, form accuracy of < 0.1 μm peak-to-valley (PV) and surface roughness of < 10.0 nm Ra is required. In order to achieve such machining precisions, it is essential to use a diamond tool in an ultra-precision diamond machine. The diamond tool has high hardness and wear resistance, can be manufactured to have sharp edges, and enables high-precision mirror-like cutting without requiring post-processing. Fig. 1(b) shows the natural single-crystal diamond tool manufactured for our

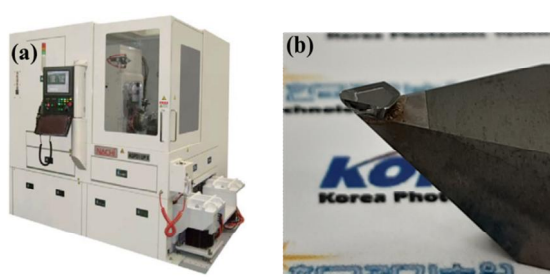

Fig. 1 (a) Ultra-precision diamond machine and (b) Diamond tool

experiments. The diamond blade is attached to a shank made of tungsten carbide using the blazing method. The cutting-edge section has a Norse radius of R 0.5 mm, rake angle of 0°, relief angle of 15°, clearance angle of 40°, and effective angle of 160°.

2.3 Workpiece Material and Measuring Instrument

Although the diamond tool has high machinability, some materials are difficult to process due to their hardness and chemical composition, e.g., carbon content in ferrous materials can chemically react with diamonds and affect its life.[10] Thus, in the machining of aspherical lens molds using the diamond tool, non-ferrous metals such as electroless nickel, brass, aluminum, beryllium, and copper are mainly used.[11] In this study, brass material was used. The form accuracy and surface roughness of the machined surface were measured and analyzed using the Form Talysurf instrument (FTS, model: PGI-840, Taylor Hobson).

3. Results and Discussion

3.1 Waviness Error by Pressure Variation of Compressed Air

The operation of the ultra-precision diamond machine requires utilities such as compressed air, coolant, and hydrostatic oil. Compressed air is needed to maintain the pressure of the vibration isolation system, operate the air-bearing-based work spindle, and spray the oil mist. The coolant is required to maintain the temperature of the machine's feed axes (X, Y, Z, and B), and the hydrostatic oil is needed to transfer the feed axis along the non-friction structured slide guideway. It is important to maintain the constant pressure and temperature of the compressed air, coolant, and hydrostatic oil introduced into the cutting machine.

Fig. 2 presents the experimental results of the cases

Table 1 Machining conditions

Material	Shape	Norse radius (mm)	Spindle speed (rpm)	Feed rate (mm/min)
Brass	Flat	R 0.5	1,000	F15.0
				F10.0
				F5.0
				F3.0
				F1.0
				F0.5

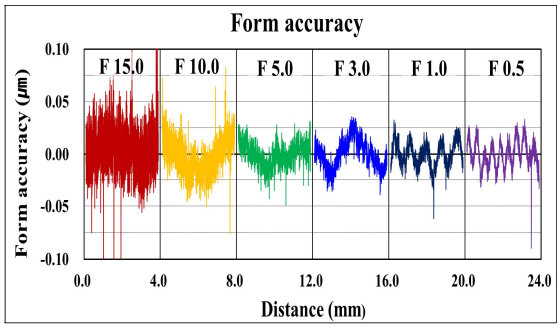

Fig. 2 The form accuracy error with waviness by pressure variation of compressed air

in which waviness error is generated owing to a pressure variation of compressed air. In experiments, plane brass workpiece with a diameter of 50 mm was used and a diamond tool with a Norse radius of R = 0.5 mm. In terms of the machining process conditions (Table 1), the machining tests were conducted by varying the feed rate as F = 15.0, 10.0, 5.0, 3.0, 1.0, and 0.5 mm/min for each 4.0 mm section from the outer skirt while the workpiece was rotating at 1,000 rpm. Fig. 2 also presents the analysis results of the machining precision obtained after the measurement of the workpiece manufactured in a plane shape. Based on the analysis results, we determined that the V-shaped waviness error is generated with a period specific to the feed rate and that this period narrows as the feed rate decreases.

This type of waviness error was estimated to occur owing to the periodic pressure variation of the compressed air introduced into the cutting machine.

The compressed air generated from the main air compressor is maintained a pressure range of 9.0-10.0 MPa over a 1 min interval. This compressed air was introduced into the cutting machine at a pressure of 6.0 MPa through four decompression regulators and a temperature and humidity control device, and distributed to the vibration isolation system, oil mist, and work spindle. From the pressure-gauge readings, we examined that the compressed air introduced into the work spindle exhibits a periodic pressure variation in the range of 5.3-5.6 MPa. This periodic pressure variation results in a location error on the Z-axis direction of the work spindle to which the workpiece is attached. Consequently, a V-shaped waviness error is generated in the machined surface of the workpiece because of the location error (dependent on the intensity of the compressed air), and furthermore, as the cutting speed decreases, the period of the waviness error gradually narrows. Pressure variations of this nature can also occur in the coolant and hydrostatic oil apart from changes in the pressure of the compressed air. The resulting location error is dependent on the pressure intensity and can result in reduced machining precision. Therefore, the regular maintenance of utilities of compressed air, coolant, and hydrostatic oil is important for improving the machining precision.

3.2 Surface Defects by External Shock

Vibration is a key factor affecting the surface roughness of the machined surface in ultra-precision machining; importantly, it is one of the variables that are difficult to control. Vibration can be generated owing to factors such as external shock, self-vibration of the cutting machine, and the chattering of the workpiece and tools. To minimize the effects of vibration transferred from the external environment, as mentioned earlier, the ultra-precision cutting machine was installed in a specially designed independent booth in a cleanroom. Furthermore, an active-type vibration isolation system that can adjust the pressure

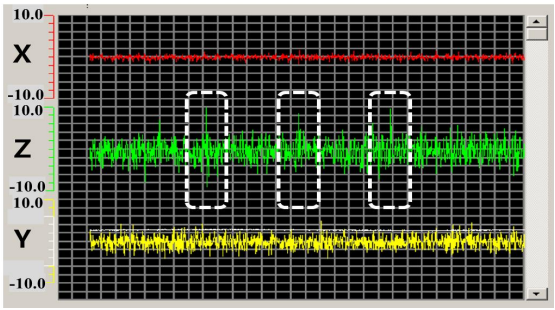

(a) Graph of 'Position Error' on machine

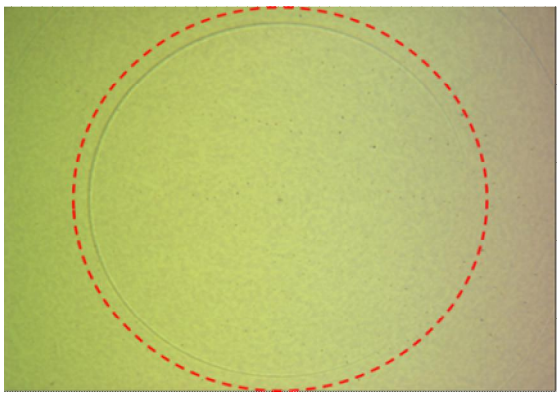

(b) Surface defect by external shock

Fig. 3 The surface defect by external shock

according to the intensity of vibration is equipped in this machine itself.

Fig. 3(a) shows the real-time position-error graph of the feed axis over 0.6 ms time intervals. In this study, this position-error variation was considered as vibration reflected by several factors. From the graph, we note that the ultra-precision cutting machine affords regular location errors of X ± 0.5 nm, Z ± 2 nm, and Y ± 1 nm in the stationary state. Over and above this error, instantaneously intensified location errors usually occur owing to external shocks, during which band-shaped surface defects can form on the machined surface (Fig. 3(b)). However, this type of surface defect can also occur if impurities or air bubbles are included in the workpiece surface; hence, it is needed to distinguish the causes of such defects through close observation.

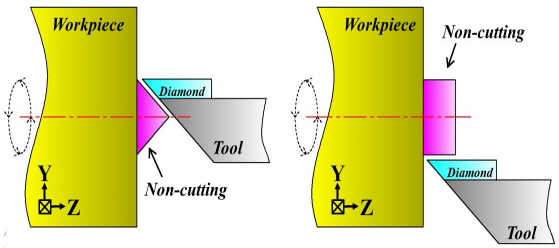

Fig. 4 Schematics of machining accuracy error by tool-height

3.3 Form Accuracy by Tool Errors

In the machining of rotationally symmetric aspherical lenses, tool error is one of the major factors leading to form accuracy error. The tool installed for machining can easily generate height error, location error along the transfer direction, and radius error in the tool-path generation process. In this study, we analyzed the various types of form accuracy errors for different types of tool errors via computer aided design (CAD) simulations.

3.3.1 Form Accuracy by Height Error

In the machining of rotationally symmetric aspherical lenses, the height of the cutting surface of the tool should align with the workpiece rotation axis. Fig. 4 shows the schematic of the machining error generated at the center of the machined surface when the tool-cutting surface does not align with the axis of rotation of the workpiece. If the height of the cutting surface of the tool is above or below the axis of rotation of the workpiece, a cone/cylinder-shaped unprocessed form error is generated at the center of the machined surface. In such a case, the shape and size of the unprocessed form needs to be analyzed, and the height of the cutting surface of the tool should be corrected such that it aligns with the rotation axis of the workpiece.

3.3.2 Form Accuracy by Location Error

It is important to ensure that the center of the tool tip radius aligns with the workpiece rotation axis. However, the tool is commonly installed after being moved in the X-axis direction, which is the transfer direction, relative to the workpiece rotation axis. Fig. 5(a) shows the schematic of the machining error generated on a concave-shaped machined surface when the center of the tool tip radius is installed after being moved along the "+X" direction relative to the workpiece rotation axis. In this case, we determined that a W-shaped machining error is generated when the cutting tool moves along the tool path. Figs. 5(b) and (c) depict the CAD-simulation-analysis-based results of the types of form accuracy errors corresponding to tool location errors along different directions during concave-shaped machining; Fig. 5(b) and (c) correspond to the cases that the tool is installed after being moved along the +X- or -X-direction relative to the workpiece rotation axis, respectively. We note that different types of form accuracy errors appear depending on the location error along the transfer direction of the installed tool. Thus, the transfer direction location error of the tool should be corrected by comparing the shape of the workpiece (concave/convex) with the form-accuracy analysis results.

3.3.3 Form Accuracy by Radius Error

In ultra-precision machining, the tool path refers to the path along which the tool moves. The tool path can be expressed using location coordinates such as (X, Z) or (X, Z, B) depending on the machine characteristics and machining method. The location coordinates of the tool path for the precise machining should be estimated after considering the tool radius. During the process of location-coordinate estimation, the tool radius is reflected as being larger or smaller than that of the actually manufactured tool.

Fig. 6(a) shows the schematic of the machining errors generated on the machined surface when the tool radius reflected in the tool path "appears" larger than that of the actual tool. Figs. 6(b) and (c) present the CAD-simulation-based analysis results of the types

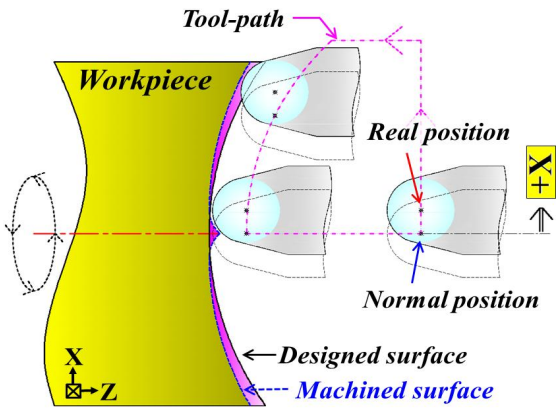

(a) Schematic of form accuracy error by the location of tool's radius center

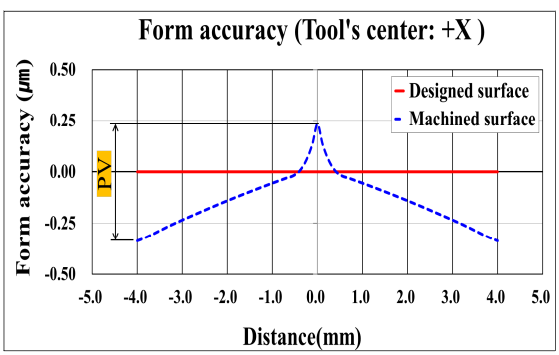

(b) A type of form accuracy error when the tool's radius center has located in +X direction

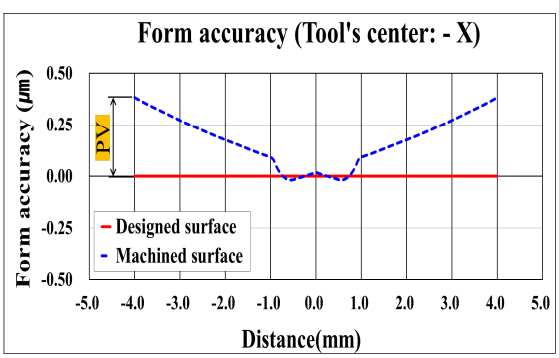

(c) A type of form accuracy error when the tool's radius center has located in -X direction

Fig. 5 Types of form accuracy error due to location error of the tool

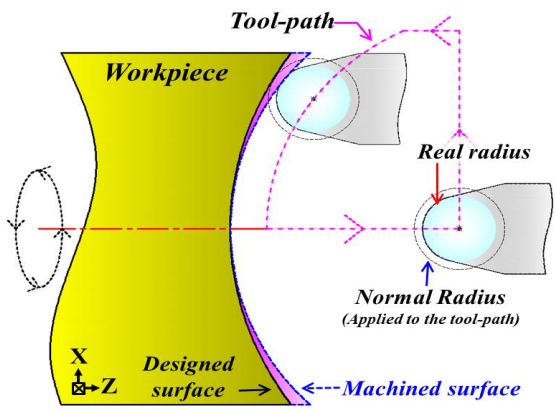

(a) Schematic of machining accuracy error by the size of tool radius

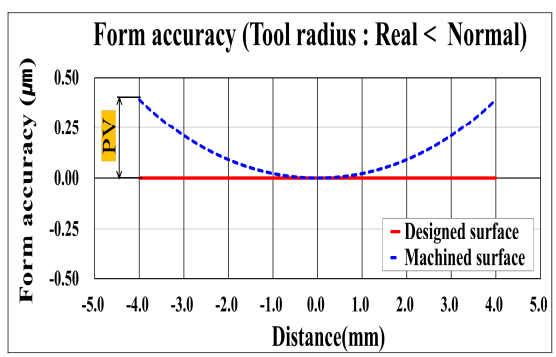

(b) A type of form accuracy error when the real tool radius is smaller

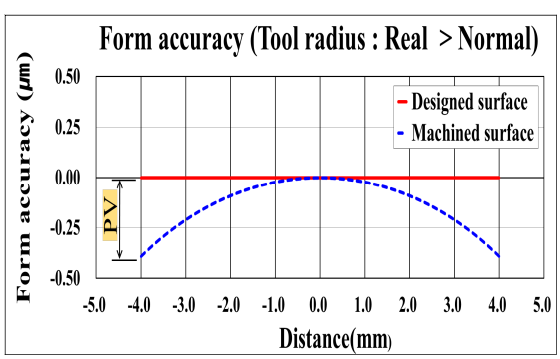

(c) A type of form accuracy error when the real tool radius is bigger

Fig. 6 Types of form accuracy error due to radius error of the tool

of form accuracy errors generated on the machined surface when the radius of the actual tool is smaller or larger than the tool radius reflected in the tool path during concave-shaped machining. From the graph, wenote that the radius-error types of the tool are different depending on the size reflected; hence, the tool radius should be corrected and the location coordinates of the tool path should be regenerated based on the analysis results.

3.4 Surface Roughness by Machining Conditions

The theoretical surface roughness of the machined surface can be calculated based on the tool radius, rotation speed, and feed rate. It is noteworthy that the surface roughness reduces as the tool radius and rotation speed increase and the feed rate decreases. In this study, we performed experiments to analyze the surface roughness of the actual machined surface under different rotation speeds and feed rates. Fig. 7 shows the image obtained by flashing a halogen light on the side of the tested workpiece. Table 2 shows the machining conditions for experiments. For the experiments, a plane-shaped brass sample with a diameter of 50 mm and a diamond tool with R = 0.5 mm were used. Prior to the experiments, planar machining was performed at a feed rate of F = 10.0 mm/min to minimize the deviation of the cutting thickness, and furthermore, a ring-shaped pattern was formed in each 3.5 mm section where the feed rate changed. In each experiment, the rotation speed was applied as 1,000 rpm, 1,250 rpm, and 1,500 rpm respectively. The feed rate was varied as F = 20.0, 15.0, 10.0, 5.0, 3.0, 1.0, and 0.5 mm/min for every 3.5 mm from the outer skirt, and the machining tests were carried out. Fig. 8 presents the analysis results of the surface roughness for different rotation speeds and feed rates. The FTS was used for the measurement and analysis, and the analysis results were presented in the form of a graph using MS-Excel.

The surface roughness was measured at a measurement speed of 0.5 mm/s and data acquisition interval of 1.0 μm and subsequently analyzed with a Gaussian filter and cut-off length of 0.0025 mm. Fig. 9(b) shows a graph analyzed based on the surface roughness of Rz. We note that the roughness of the machined surface tends to improve as the rotation speed of the workpiece increases and the feed rate decreases. However, we also note a significant difference between the surface roughness values of the machined surface for different rotation speeds at feed rates of F > 10.0 mm/min; at feed rates of F < 5.0 mm/min, the surface roughness is not significantly affected by the rotation speed. The optimum surface roughness that could be achieved in our experiments was Rz = 0.0105 μm at a rotation speed of 1,000 rpm and feed rate of F = 1.0 mm/min.

3.5 Effects of Tool Wear and Vibration

Although the diamond tool exhibits high hardness

Table 2 Machining conditions

Material	Shape	Norse radius (mm)	Spindle speed (rpm)	Feed rate (mm/min)
Brass	Flat	R 0.5	1,000	F20.0
				F15.0
				F10.0
			1,250	F5.0
				F3.0
				F1.0
			1,500	F0.5

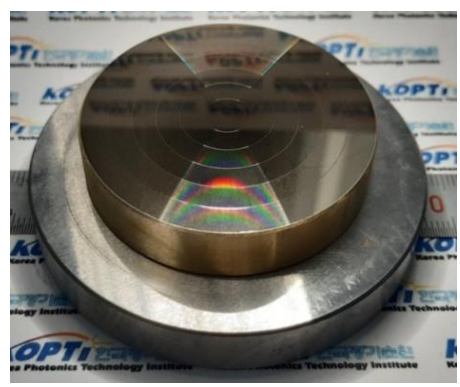

Fig. 7 Workpiece

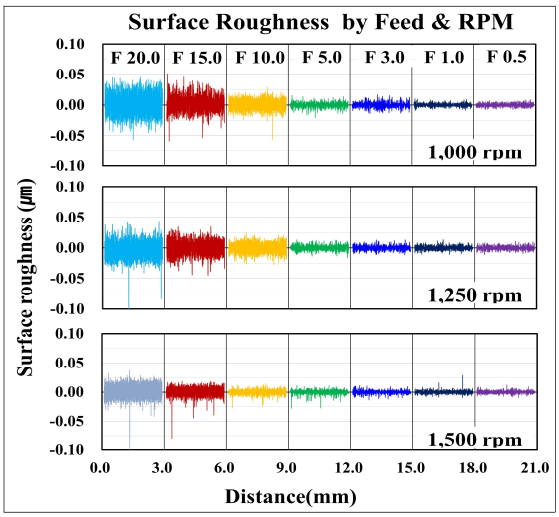

(a) Surface roughness by Feed rate & RPM

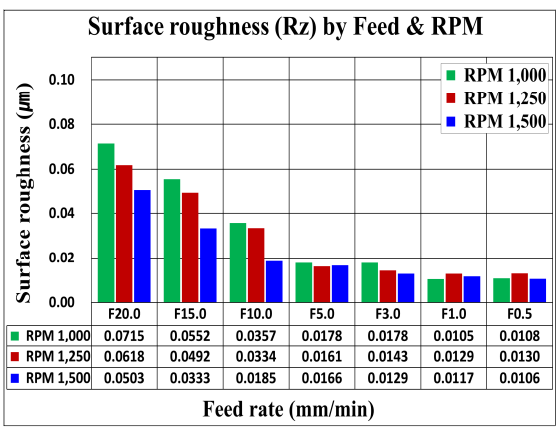

	F20.0	F15.0	F10.0	F5.0	F3.0	F1.0	F0.5
RPM 1,000	0.0715	0.0552	0.0357	0.0178	0.0178	0.0105	0.0108
RPM 1,250	0.0618	0.0492	0.0334	0.0161	0.0143	0.0129	0.0130
RPM 1,500	0.0503	0.0333	0.0185	0.0166	0.0129	0.0117	0.0106

(b) Surface roughness of 'Rz'

Fig. 8 Surface roughness by Feed rate & RPM

and machinability, it naturally wears as usage time increases. In the aforementioned experimental results concerning the surface roughness for different rotation speeds and feed rates, we found that it is difficult to achieve a surface roughness of Rz < 0.01 μm. In this study, we attributed this limit to tool wear and vibration, and consequently, we conducted experiments to validate this assumption.

Fig. 9 presents the experimental results relating to the effects of tool wear on the surface roughness. The graph compares the theoretical surface roughness and actual surface roughness of the surface machined by applying 1 and 3 revolutions. The experiments were carried out at the rotation speed of 1,000 rpm with the tool radius set to R = 0.5 mm and the feed rate being varied for each 3.5 mm section. Based on the experimental results, we note that the surface roughness gradually reduces as the feed rate decreases. However, the roughness of the actually machined surface is significantly different from the theoretical surface roughness under the machining conditions corresponding to F < 5.0 mm/min. In particular, when analyzing the machining conditions corresponding to F = 1.0 and F = 0.5 mm/min (corresponding to a theoretical surface roughness of ~ 0), the actual surface roughness by 1 revolution was Rz ~ 0.01 μm while that of the surface machined by 3 revolutions was Rz ~ 0.02 μm. These results indicate that tool wear affects the machined surface roughness by a Rz ~ 0.01 μm.

Fig. 10 presents the experimental analysis results relating to vibration due to chattering at different rotation speeds of the workpiece. These experiments were conducted by attaching the workpiece and increasing the rotation speed, and the results were presented as a graph created using MS-Excel based on the position-error data of the ultra-precision cutting machine. From the graph, we note that the vibration along the X- and Y-axes due to chattering tends to gradually increase with an increase in the rotation speed. However, chattering along the Z-axis exhibits a constant value of ~ 10 nm regardless of the rotation speed. Moreover, even at low rotation speeds, a larger vibration is generated because of external shock and other factors. After reanalyzing the experimental results shown in Figs. 8 and 9 based on these results, we estimated that the resulting surface roughness that deviates from the predicted values is probably due to vibration effects. Therefore, to achieve optimum machining precision, the effects of tool wear and vibration need to be minimized.

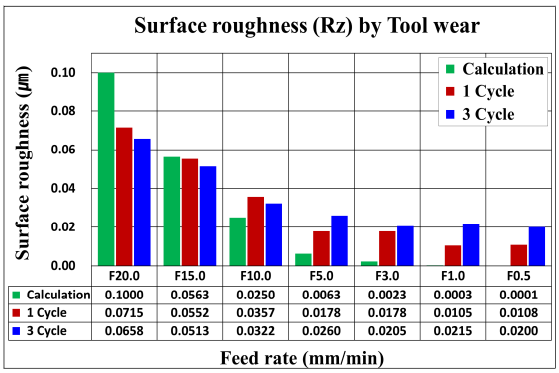

Fig. 9 Surface roughness by tool wear

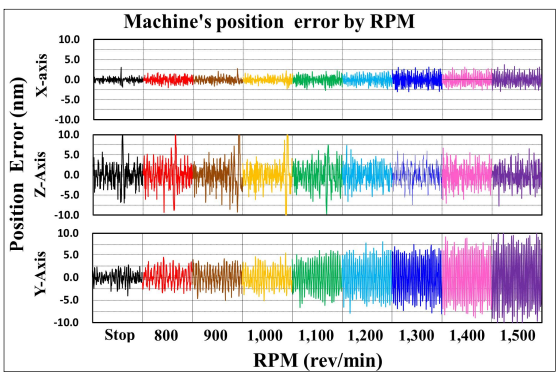

Fig. 10 Vibration by work-spindle's rotational speed

4. Conclusions

In this study, we analyzed the representative factors affecting the machining precision in diamond-tool-based ultra-precision machining, and we performed experiments to analyze the types of machining errors related to such factors. The representative factors that reduce the machining accuracy are pressure variation of compressed air, external shock, tool errors, machining conditions, tool wear, and vibration due to the rotation speed of the workpiece. Our findings can be summarized as follows:

1. The pressure variation of compressed air generates a location error along the Z-axis direction when the air-bearing-based work spindle rotates, thereby leading to a waviness error on the machined surface.
2. The external shock causes position error, resulting in the formation of ring-shaped surface defects on the machined surface.
3. The diamond tool installed for the experiments commonly exhibits height errors, feed-direction location errors, and radius errors during tool-path calculation. Through CAD simulations, we found that different types of form accuracy errors are generated on the machined surface depending on the types of tool errors.
4. The surface roughness shows a tendency to improve with increasing rotation speed and decreasing feed rate. In particular, under the effects of tool wear and vibration, an actual surface roughness of Rz = 0.0105 μm could be achieved at a rotation speed of 1,000 rpm and feed rate of F = 1.0 mm/min.

Acknowledgment

"This work was supported by the Technology Innovation Program (Development of GMP Equipment and Manufacturing Technology for High Temperature Forming, # 20010775), funded by the Ministry of Trade, Industry & Energy (MOTIE, Korea).
"This work was supported by the Academic Research Fund [2021-1446] of Chonnam National University."

REFERENCES

1. Kim, Y. B., Park, J., Lee, W. S., and Lee, J. K., "Fabrication of Microlens Array by the Tilted Milling Method to Improve the Surface Morphology," Materials and Manufacturing Processes, 2021.
2. Lee, D. K., Kim, H. U., Cha, D. H., Lee, H. S., Kim, H. J., et al., "A Study on Thermal Deformation Compensation in the Molding of Aspheric Glass Lenses," Journal of the Korean

Society for Precision Engineering, Vol. 27, No. 5, pp. 22-26, 2010.

3. Hatefi, S. and Abou-El-Hossein, K., "Review of Single-point Diamond Turning Process in Terms of Ultra-precision Optical Surface Roughness," The International Journal of Advanced Manufacturing Technology, Vol. 106, No. 5, pp. 2167-2187, 2020.
4. Kim, M. S., Kim, J. T., Park, S W., Jeong, D. U., et al., "Effect of Unbalance on Vibration and Machining of Al6061 Aluminum Alloy in Precision Rotator," Journal of the Korean Society of Manufacturing Process Engineers, Vol. 20 No. 3 pp. 76-82, 2021.
5. Mishra, V., Khan, G. S., Chattopadhyay, K. D., Nand, K., and Sarepaka, R. V., "Effects of Tool Overhang on Selection of Machining Parameters and Surface Finish During Diamond Turning," Measurement, Vol. 55, pp. 353-361. 2014.
6. Wang, H., To, S., and Chan, C. Y., "Investigation on the Influence of Tool-tip Vibration on Surface Roughness and its Representative Measurement in Ultra-precision Diamond Turning," International Journal of Machine Tools and Manufacture, Vol. 69, pp. 20-29, 2013.
7. Kim, Y. B., Hwang, Y., An, J. H., Kim, J. H., Kim, H. J., et al, "Improvement in Surface Roughness by Multi Point B Axis Control Method in Diamond Turning Machine," Journal of the Korean Society for Precision Engineering, Vol. 32, No. 11, pp. 983-988, 2015.
8. Kim, Y. J., Choi, H. J., Lee, K. H., Yeo, W. J., Jeong, J. Y., et al, "A Study on the Characteristics of Ultra-Precision Surface Cutting of the Mold Material (STAVAX) for the Development of Large Satellite Lens," Journal of the Korean Society for Precision Engineering, Vol. 37, No. 11, pp. 819-825, 2020.
9. Mishra, V., Khatri, N., Nand, K., Singh, K., and V Sarepaka, R, "Experimental investigation on uncontrollable parameters for surface finish during diamond turning," Materials and Manufacturing Processes, Vol. 30, No. 2, pp. 232-240, 2015.
10. Mishra, V., Garg, H., Karar, V., and Khan, G. S., Ultra-precision Diamond Turning Process, Springer, 2019.
11. Lee, G. I., & Kim, J. Y. "A Study on Heat Generation and Machining Accuracy According to Material of Ultra-precision Machining," Journal of the Korean Society of Manufacturing Process Engineers, Vol. 17, No. 1, pp. 63-68, 2018.